Tracking down protein-protein interaction *via* FRET-system using site-specific thiol-labeling

B. Söveges,[a] T. Imre,[b] Á. L. Póti,[c] P. Sok,[c] Zs. Kele,[a] A. Alexa,[c] P. Kele [a] and K. Németh*[a]

a. Research Centre for Natural Sciences of the Hungarian Academy of Sciences, Institute of Organic Chemistry, Chemical Biology Research Group, H-1117 Budapest, Magyar tudósok krt. 2, Hungary. E-mail: nemeth.krisztina@ttk.mta.hu; Tel: +36 1 382 6659.

b. Research Centre for Natural Sciences of Hungarian Academy of Sciences, Instrumentation Center, MS Metabolomics Research Group; H-1117 Budapest, Magyar tudósok krt. 2., Hungary.

c. Research Centre for Natural Sciences of the Hungarian Academy of Sciences, Institute of Enzymology, Protein Research Group, H-1117 Budapest, Magyar tudósok krt. 2, Hungary.

Supporting information

Content

S1. Mass spectra of the intact protein

The molecular weights of the intact unmodified and labeled $p38^{C162S}$ and MK2 were identified using a Triple TOF 5600+ hybrid Quadrupole-TOF LC/MS/MS system (Sciex, Singapore, Woodlands) equipped with a DuoSpray IonSource coupled with a Perkin Elmer Series 200 micro-LC system (Massachusetts, USA) consisting of binary pump and an autosampler. Data acquisition and processing were performed using Analyst TF software version 1.7.1 (AB Sciex Instruments, CA, USA). Chromatographic separation was achieved by Phenomenex Aeris Widepore XB-C8 (50 mm × 2.1 mm, 3.6 µm, 200 Å) HPLC column. Sample was eluted in gradient elution mode using solvent A (0.1% formic acid in water) and solvent B (0.1% formic acid in CH_3CN). The initial condition was 20% B, followed by a linear gradient reaching 90% B within 5 min, from 5 to 6 min 90% B was retained; and from 6 to 6.5 min back to initial condition with 20% eluent B and kept from 6.5 to 9.5 min. Flow rate was set to 0.25 ml/min. The column temperature was set at room temperature and the injection volume was 5 µl. Nitrogen was used as the nebulizer gas (GS1), heater gas (GS2), and curtain gas with the optimum values set at 30, 30 and 35 (arbitrary units), respectively. Data were acquired in positive electrospray mode in the mass range of m/z=500 to 2500, with 1 s accumulation time. The source temperature was 350°C and the spray voltage was set to 5500 V. Declustering potential value was set to 80 V. Peak View Software™ V.2.2 (version 2.2, Sciex, Redwood City, CA, USA) was used for deconvoluting the raw electrospray data to obtain the neutral molecular masses.

In order to demonstrate thiol selectivity of our heterobifunctional linker GSH–linker **10** conjugate was studied in MS-MS mode, with mass range of m/z=100 to 1500 and 1 s accumulation time. Declustering potential value was set to 80 V, and collision energy to 35 eV. The presence of ions m/z=458 and m/z=558 proves that the linker binds to sulfur not to amino nitrogen (**Fig. S1**). (These fragments can only be formed when the linker binds to the sulfur atom of cysteine.) The high-resolution data support the elemental composition of these fragment ions.

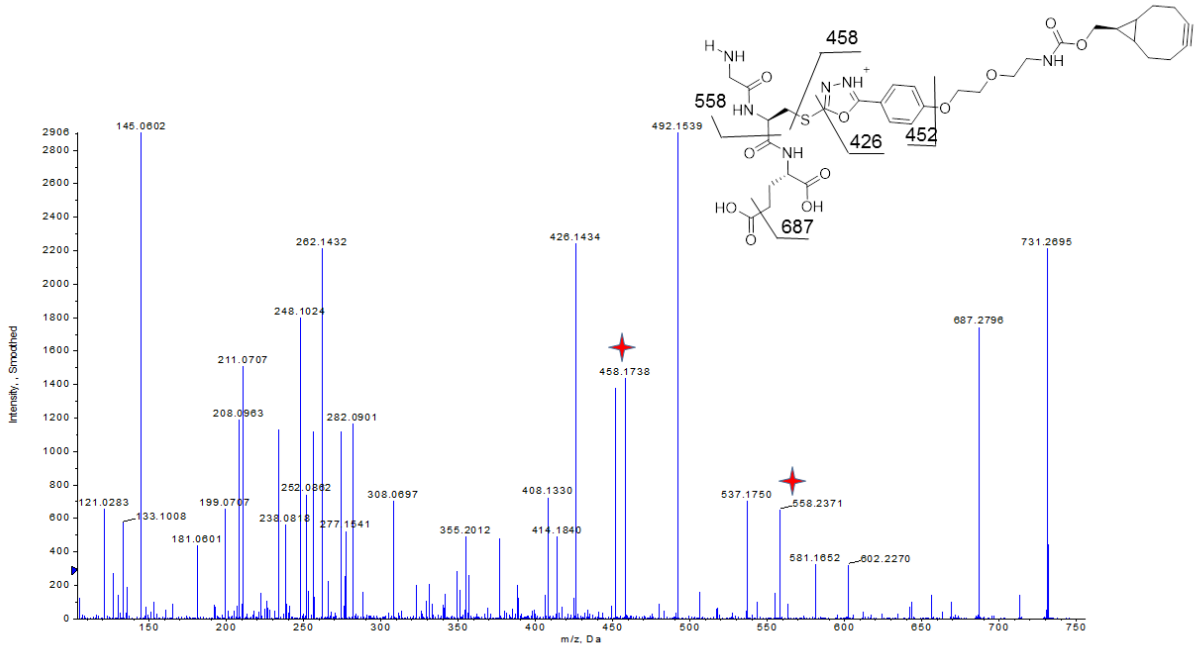

Fig. S1. ESI MS-MS spectra of GSH–linker **10** conjugate.

Efficiency of fluorescent labeling process was verified by intact protein MS. After deconvolution of protein spectra, the measured protein mass for sample p38^{C162S} was 43902 Da (**Fig. S2**). The spectrum contained several adduct peaks as well, which gave additional peaks in automated deconvolution. After incubation (10 min at room temperature) of the intact protein (60 µM) with the heterobifunctional linker **10** (120 µM) the peak of the untreated protein disappeared and the mono-conjugated species at 44325 Da appeared (**Fig. S3**). 100% conversion was detected after 10 minutes of addition of dye **11** (240 µM). This peak at 44705 Da corresponds to the mono-derivatized form of p38^{C162S} (**Fig. S4**). In case of dyes **12–15** the same efficiency was observed (**Fig. S5–8**) however, a negligible amount of double-conjugated variant could also be detected (<10%).

In case of MK2 protein the untreated form was detected at 42821 Da molecular mass (**Fig. S9**). Upon addition of the linker **10** in two-fold molar excess, the peak of the original protein diminished and two new peaks evolved corresponding to the mono- and double-derivatized species of MK2 protein (**Fig. S10**). Fluorescent labeling with dye **12** showed similar results as demonstrated for p38^{C162S}.

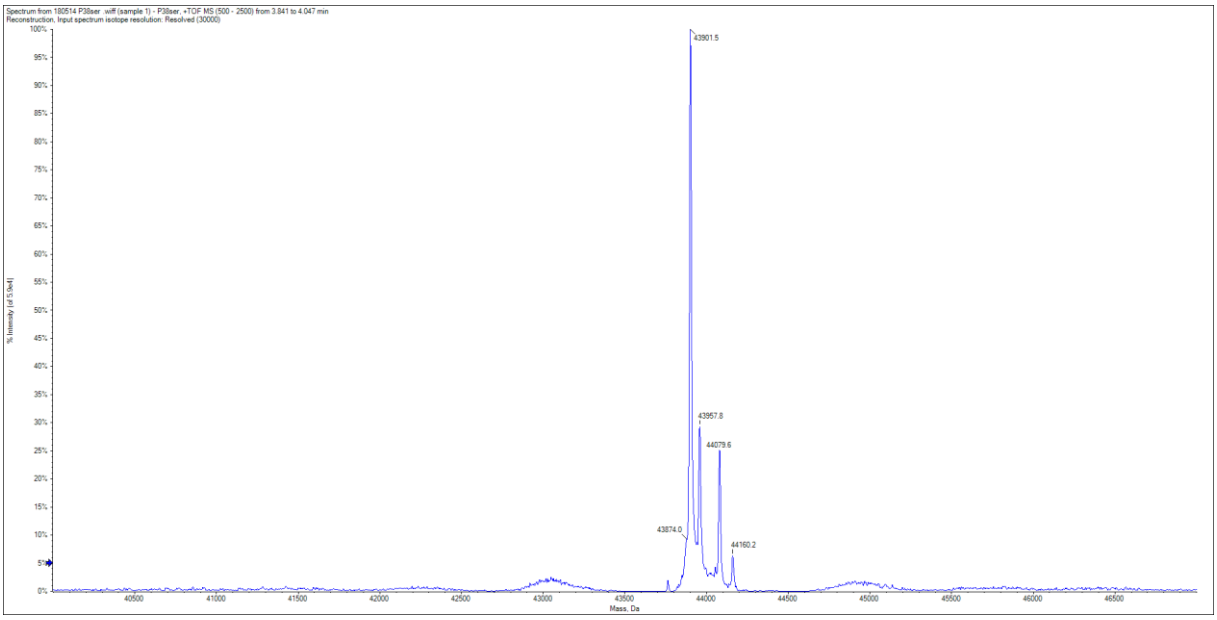

Fig. S2. Deconvoluted ESI-MS spectrum of the intact and unmodified p38^{C162S}.

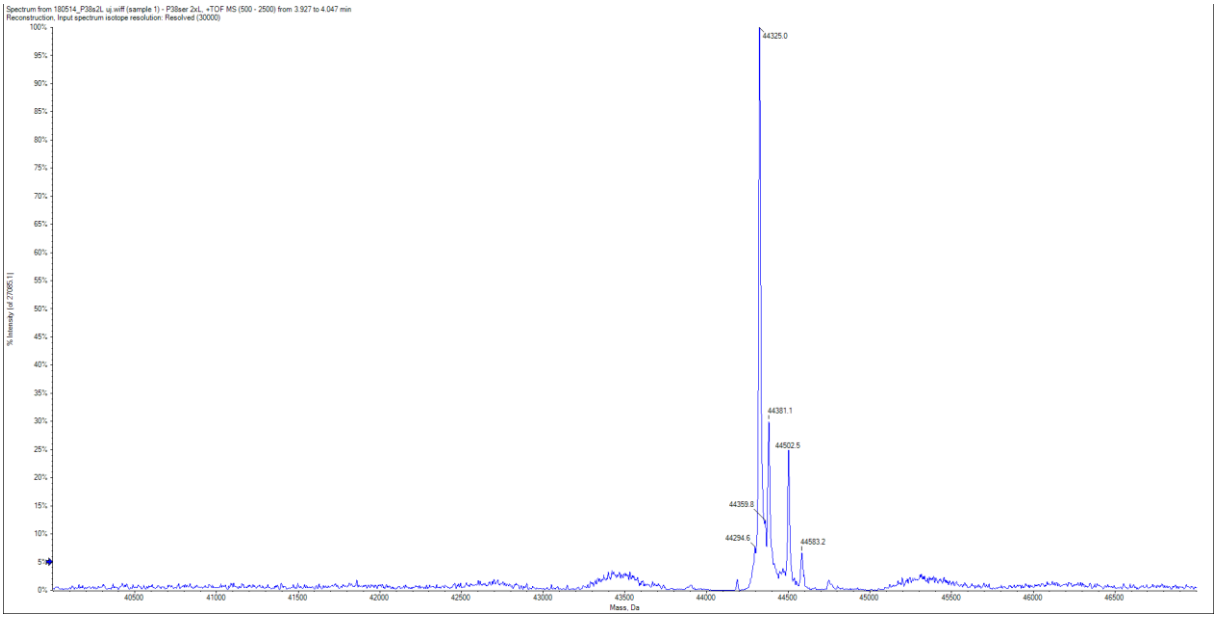

Fig. S3. Deconvoluted ESI-MS spectrum of the linker **10** conjugated p38^{C162S}.

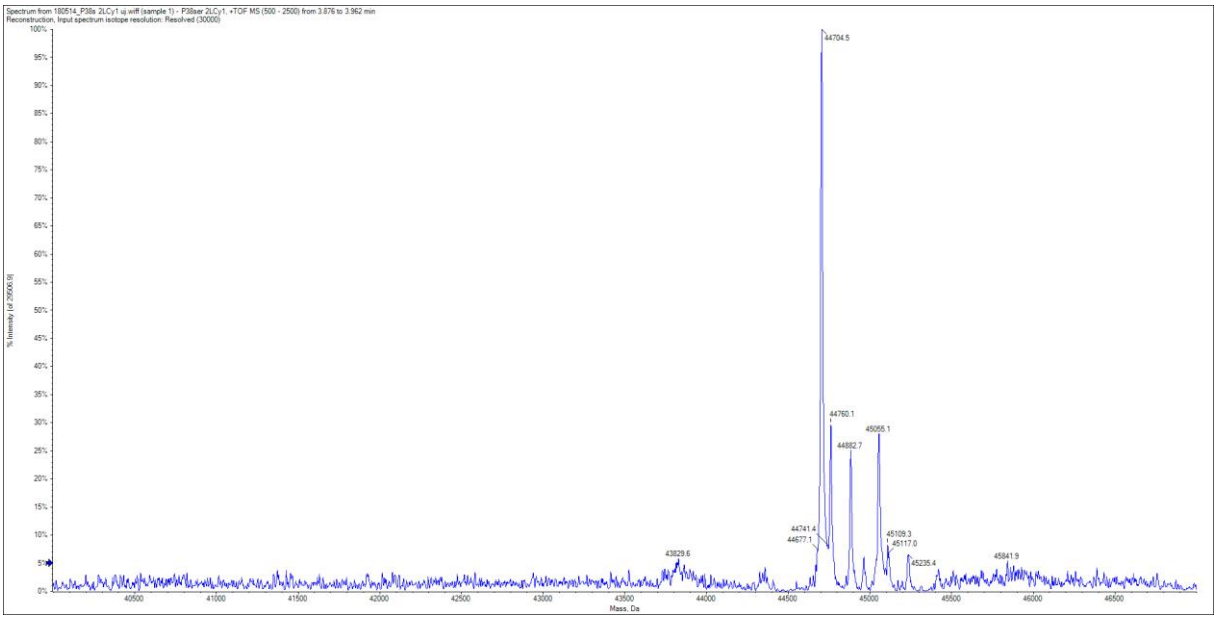

Fig. S4. Deconvoluted ESI-MS spectrum of the linker **10** conjugated and the dye **11** modified p38^{C162S}.

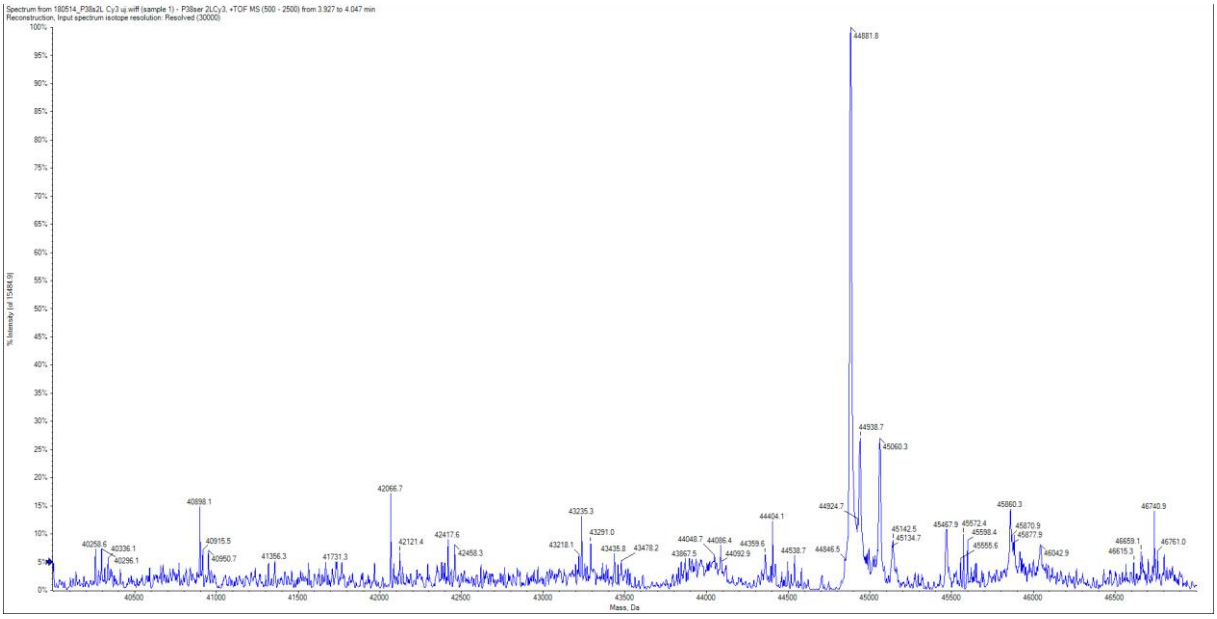

Fig. S5. Deconvoluted ESI-MS spectrum of the linker **10** conjugated and the dye **12** modified p38^{C162S}.

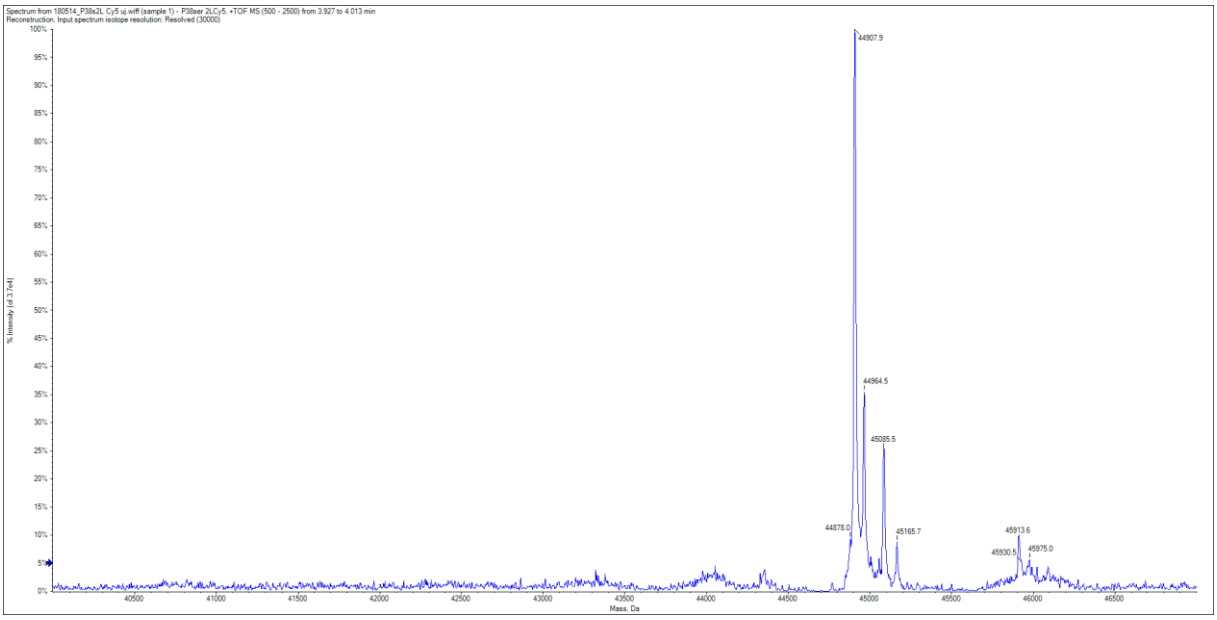

Fig. S6. Deconvoluted ESI-MS spectrum of the linker **10** conjugated and the dye **13** modified p38^{C162S}.

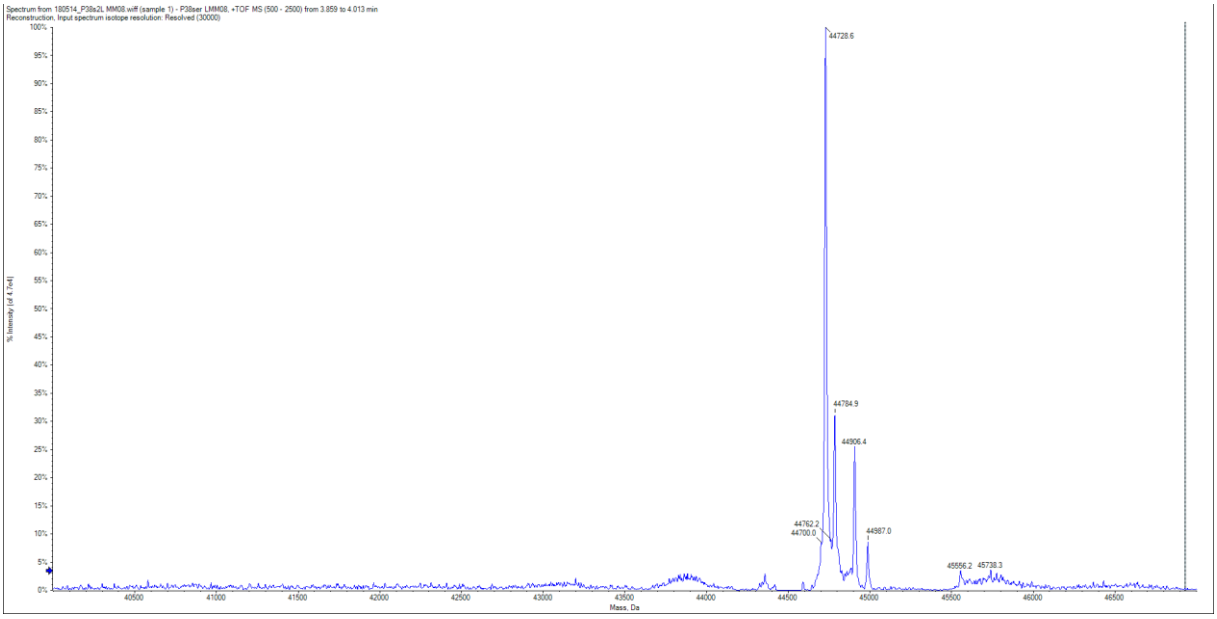

Fig. S7. Deconvoluted ESI-MS spectrum of the linker **10** conjugated and the dye **14** modified p38^{C162S}.

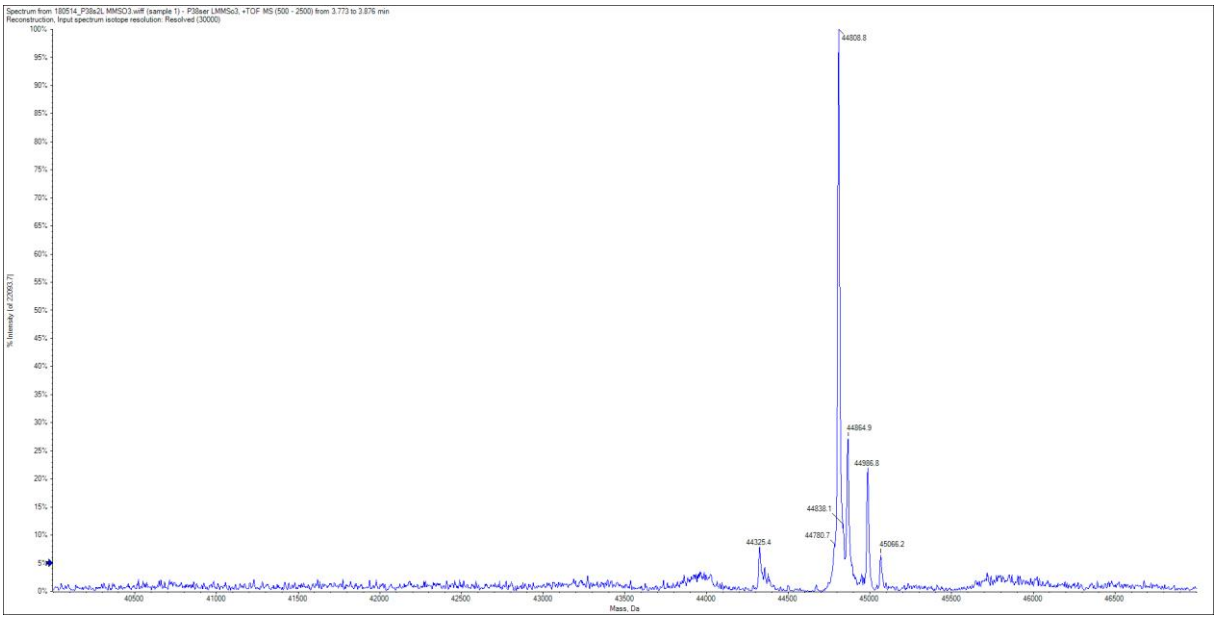

Fig. S8. Deconvoluted ESI-MS spectrum of the linker **10** conjugated and the dye **15** modified p38^{C162S}.

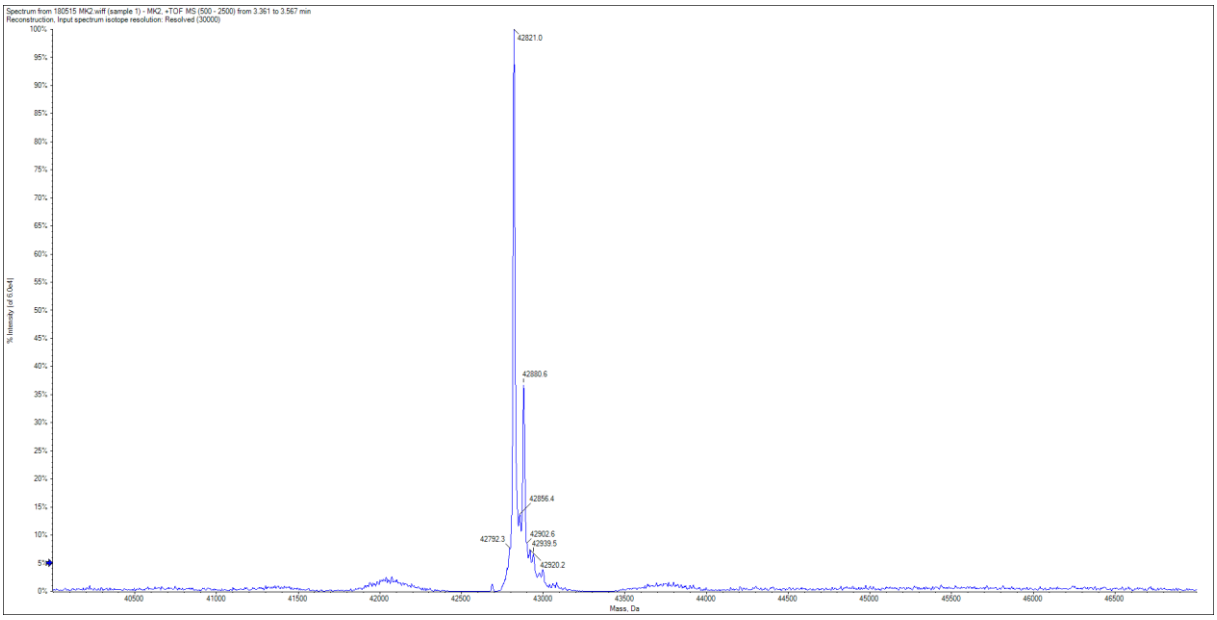

Fig. S9. Deconvoluted ESI-MS spectrum of the intact and unmodified MK2 protein.

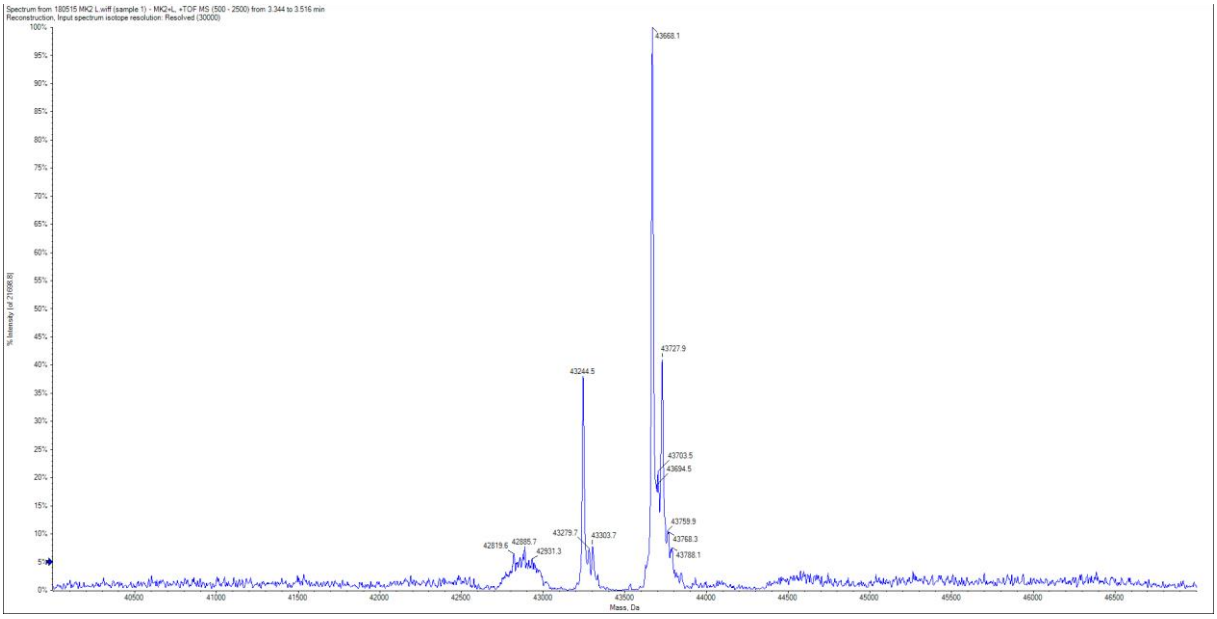

Fig. S10. Deconvoluted ESI-MS spectrum of the linker **10** conjugated MK2 protein.

S2. Identification of labeling site

In order to identify the labeling site of $p38^{C162S}$ and MK2 protein the Cys containing peptide fragments – obtained by tryptic digestion of the proteins – were investigated by LC-MS/MS. Untreated and derivatized samples were compared. In $p38^{C162S}$ the Cys 119 was labeled by compound **9** (**Fig. S11**). The possible labeling site of MK2 could be the Cys 98, 140, and 224 according to the ASA values (**Table S1**). The decrease of the amount of the peptide fragments in the conjugated samples given in the percentage of the referring untreated ones was significant in the case of Cys 224 (96%) and Cys 98 (69%) (**Table S2**).

Sample preparation for the tryptic digestion. The method for proteolysis was adapted from that developed previously for AGP.[1] Briefly, 50 µL of MK2 and p38 (2 mg/mL, 50 µM, 2.5 nmol) with or without pretreatment and 10 µL 0.2% (w/v) RapiGest SF solution buffered with 50 mM NH_4HCO_3 were mixed. 2 µL of 45 mM DTT in 100 mM NH_4HCO_3 were added and kept at 37.5°C for 30 min. After cooling the sample to room temperature, 2.5 µL of 100 mM iodoacetamide in 100 mM NH_4HCO_3 were added and placed in the dark for 30 min. The reduced and alkylated protein was then digested by 5 µL (2 mg/mL) trypsin (the enzyme to protein ratio was 1/10). The sample was incubated overnight at 37°C.

Sample preparation for mass spectrometry. To degrade the surfactant, 7 µL of formic acid (500 mM) solution was added to the digested protein sample to have the final concentration between 30 and 50 mM (pH ≈ 2) and was incubated at 37°C for 45 min. For LC-MS analysis the acid treated sample was centrifuged for 10 min at 13 000 rpm.

LC-MS/MS measurements of tryptic digest of p38 and MK2. QTRAP 6500 triple quadruple – linear ion trap mass spectrometer, equipped with a Turbo V source in electrospray mode (AB Sciex, CA, USA) and a Perkin Elmer Series 200 micro LC system (Massachusetts, USA) was used for LC-MS/MS analysis. Data acquisition and processing were performed using Analyst software version 1.6.2 (AB Sciex Instruments, CA, USA). Chromatographic separation was achieved by using the Vydac 218 TP52 Protein & Peptide C_{18} column (250 mm × 2.1 mm, 5 µm). The sample was eluted with a gradient of solvent A (0.1% formic acid in water) and solvent B (0.1% formic acid in CH_3CN). The flow rate was set to 0.2 mL min^{-1}. The initial conditions for separation were 5% B for 3 min, followed by a linear gradient to 25% B by 27 min (from 3 to 30 min) and from 30 to 40 min to 90%. Then from 40 to 45 min 90% B is retained; from 45 to 50 min back to the initial conditions with 5% eluent B retained to 53 min. The injection volume was 10 µL (300 pmol on the column). Information Dependent Acquisiton (IDA) LC-MS/MS experiment was carried out to identify the modified tryptic MK2 and p38 peptide fragments. Enhanced MS scan (EMS) was applied as survey scan and enhanced product ion (EPI) was the dependent scan. The collision energy in EPI experiments was set to rolling collision energy mode, where the actual value was set on the basis of the mass and charge state of the selected ion. Further IDA criteria: ions greater than 400.000 m/z, which exceeds 106 counts, exclude former target ions for 30 seconds after 2 occurrence(s). In EMS and in EPI mode the scan rate was 1000 Da/s as well. Nitrogen was used as the nebulizer gas (GS1), heater gas (GS2), and curtain gas with the optimum values set at 50, 40 and 40 (arbitrary units). The source temperature was 350°C and the ion spray

voltage was set to 5000 V. Declustering potential value was set to 150 V. GPMAW 4.2. software and ProteinProspector (http://prospector.ucsf.edu/prospector/mshome.htm) was used to analyse the large number of MS-MS spectra and identify the modified tryptic MK2 and p38 peptides.

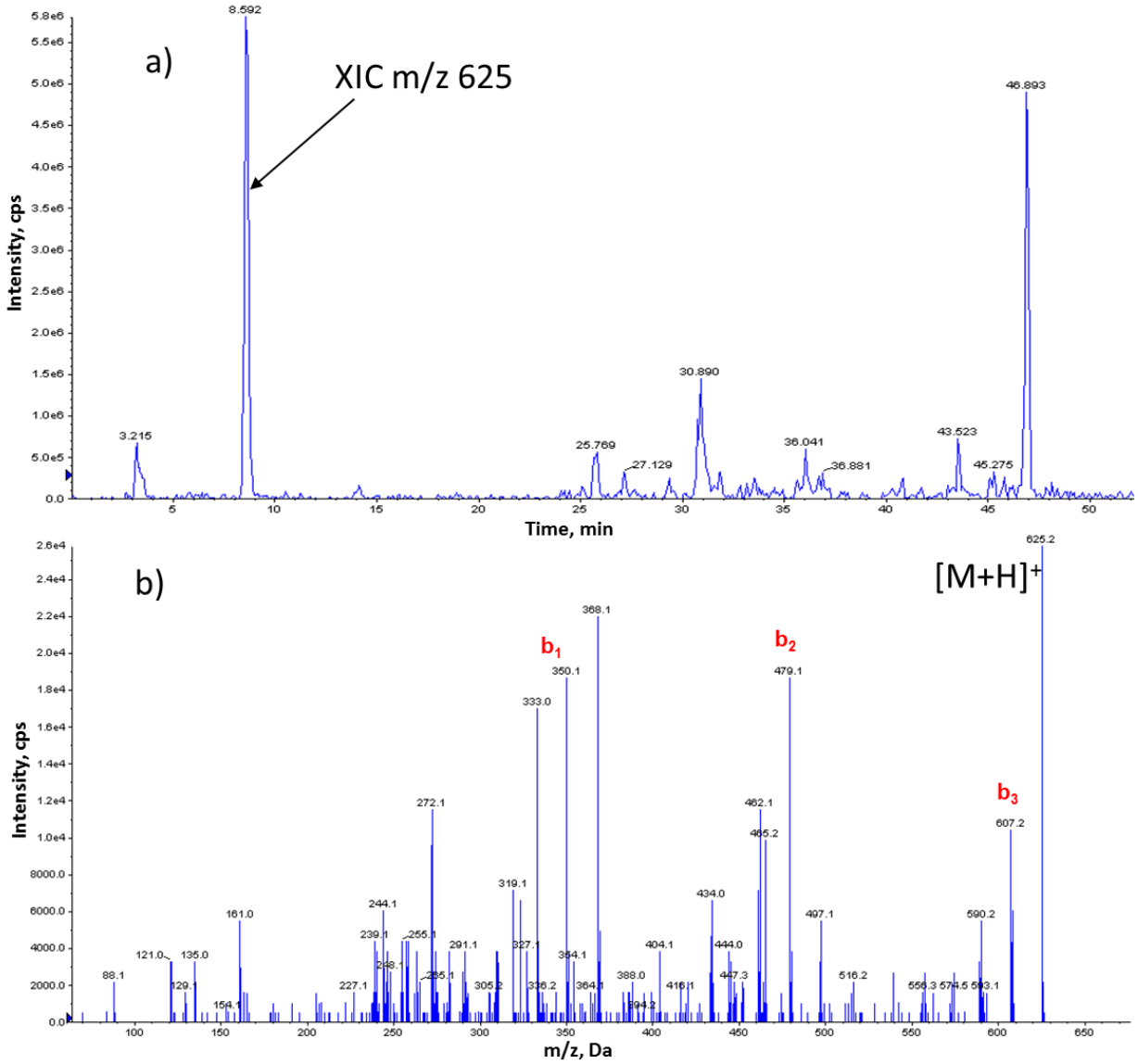

Fig. S11. a) Selected ion chromatogram (XIC) of *m/z* 625^{+} $p38^{C162S}$ [119-121] peptide fragment conjugated with compound **9**; **b)** MS/MS mass spectrum of $p38^{C162S}$ [119-121] peptide fragment conjugated with compound **9**.

S3. LC-MS analysis of Cy3-labeled pepMK2

A Sciex 6500 QTRAP triple quadrupole – linear ion trap mass spectrometer, equipped with a Turbo V Source in electrospray mode (Sciex, CA, USA) and a Perkin Elmer Series 200 micro LC system (Massachusetts, USA) consisting of binary pump and an autosampler was used for LC–MS analysis. Data acquisition and processing were performed using Analyst software version 1.6.2 (AB Sciex Instruments, CA, USA). Chromatographic separation was achieved by Purospher STAR RP-18 endcapped (55 mm × 2.1mm, 3µm) LiChocart ® 55-2 HPLC Cartridge. Sample was eluted with gradient elution using solvent A (0.1% formic acid in water) and solvent B (0.1% formic acid in CH_3CN). Flow rate was set to 0.5 mL/min. The initial condition was 5% B for 2 min, followed by a linear gradient to 95% B by 4 min, from 6 to 8 min 95% B was retained; and from 8 to 8.5 min back to initial condition with 5% eluent B and retained to 14 min. The column temperature was kept at room temperature and the injection volume was 10 µL. Nitrogen was used as the nebulizer gas (GS1), heater gas (GS2), and curtain gas with the optimum values set at 35, 45 and 45 (arbitrary units). Data were acquired in positive ionization mode from m/z=100 to 2000 in 1.7 sec. The source temperature was 450°C and the spray voltage was set at 5000 V. Declustering potential value was set to 150 V.

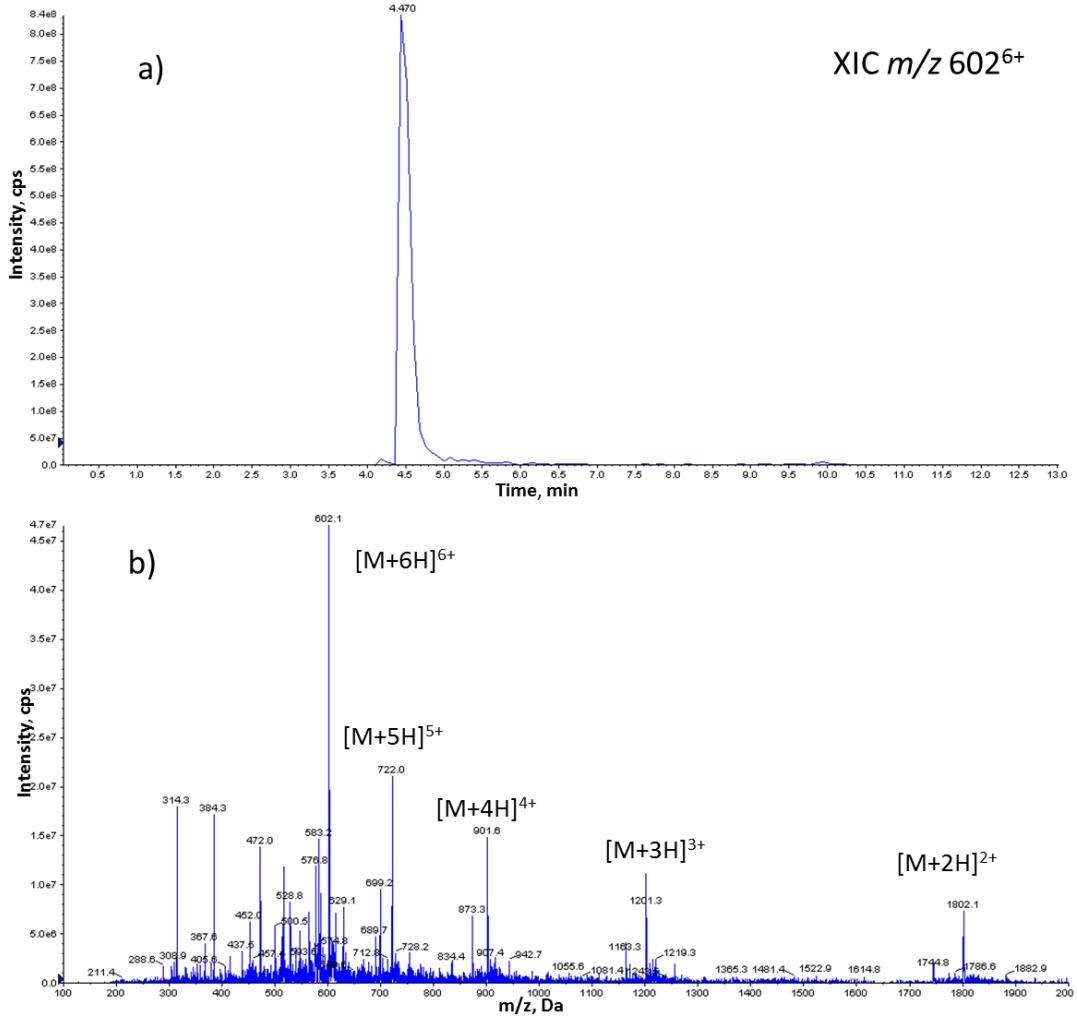

Figure S12. a) Selected ion chromatogram (XIC) of m/z 602 $[M+6H]^{6+}$ ion of Cy3-labeled pepMK2; **b)** ESI mass spectrum of Cy3-labeled pepMK2 (MW=3602).

S3. Accessible surface area calculations

Table S1. The solvent accessible surface area of the cysteines of p38^{C162S} and MK2 based on the calculations of the online prediction toolkit (http://cib.cf.ocha.ac.jp/bitool/ASA/). The most accessible cysteines are highlighted.

Protein	PDB ID	Cys	ASA	RSA
p38^{C162S}	2Y8O	39	1	0.01
		119	**103**	**0.62**
		211	2	0.01
MK2	2OZA	**98**	**45**	**0.32**
		114	5	0.03
		133	14	0.10
		140	35	0.25
		224	**110**	**0.77**
		244	3	0.02
		258	5	0.04

Table S2. Site specific labeling of linker **10** on MK2 protein.

	Peptide fragment	**Cys position**	**Untreated MK2**	**Cy3-conjugated MK2**	**Remaining non-derivatized form (%)**
			Normalized intensity		
1	94-100	98	0.619	0.193	31
2	101-132	114	0.187	0.169	90
3	133-149	133; 140	0.033	0.028	85
4	213-239	224	0.700	0.028	4

S4. Evaluation of non-specific labeling

p38 protein was incubated with four-fold excess of the fluorescent dyes with or without the pretreatment of the heterobifunctional linker **10**. After purification the fluorescent intensities of the samples were measured. The ratios of the non-specific (non-covalent) association of the fluorescent dyes given in the percentage of the specific ones was negligible since did not exceeded 7% (**Table S3**).

Table S3. Ratio of the aspecific labeling of $p38^{C162S}$ with linker **10** and the fluorescent dyes. The fluorescence intensity of the different dyes was measured at the following wavelengths ($\lambda_{exc}/\lambda_{em}$ in nm **11**: 434/482; **12**: 580/600; **13**: 515/602; **14**: 530/630; **15**: 670/692).

Dye	**Fluorescence intensity (RFU)**		**%**
	*with **10***	*without **10***	
11	131733	8515	6.5
12	34462	574	1.7
13	86334	38	0.0
14	19164	463	2.4
15	6787	44	0.6

S5. Identification of the FRET-pair dyes

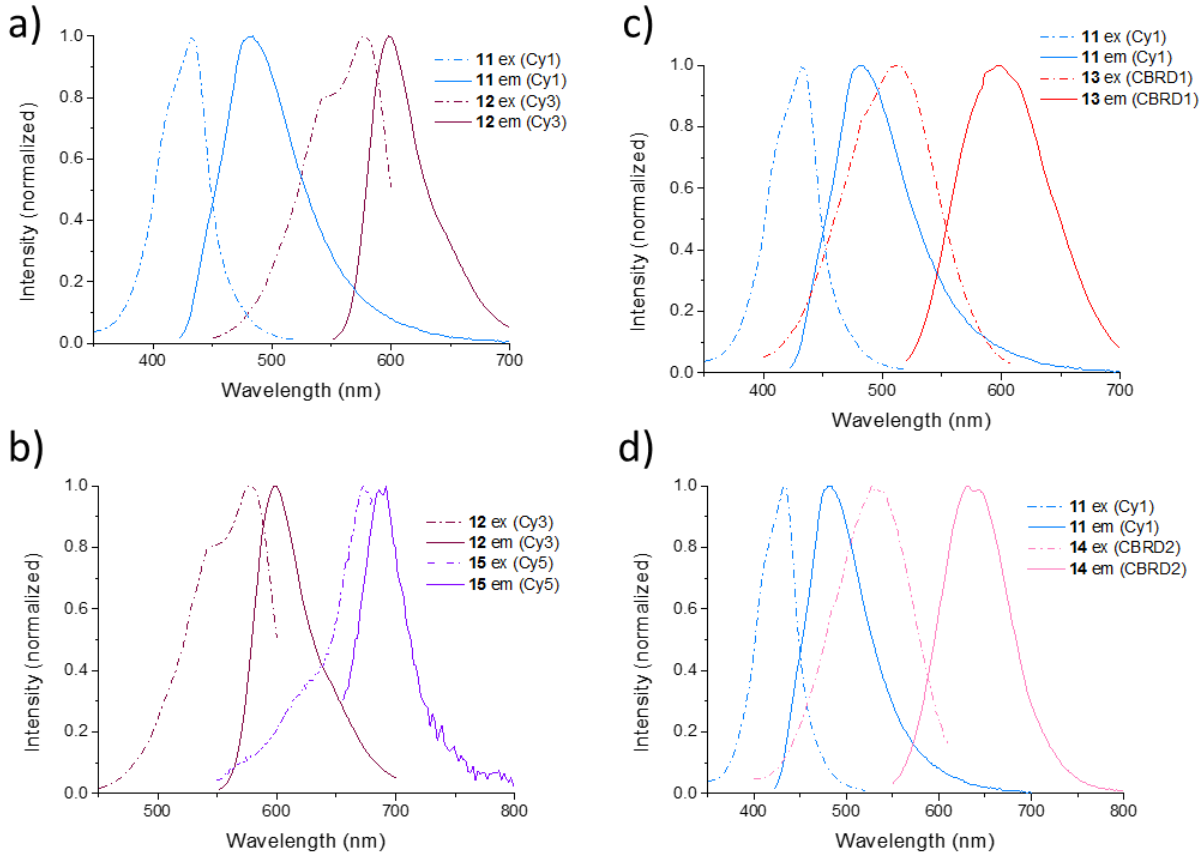

Fig. S13. The excitation and emission spectra of the possible FRET-pair dyes.

S6. Evaluation of K_d values

K_d was calculated in Originlab sofware (ver.9) using non-linear regression according to the following equation:

$$I = I_{min} + \frac{(I_{max} - I_{\min}) \cdot \left(T_0 + K_0 + K_d - \sqrt{(T_0 + K_0 + K_d)^2 - 4T_0K_0}\right)}{2K_0}$$

where

I_{min} – the FRET efficiency at the minimum point,

I_{max} – the FRET efficiency at the maximum point,

T_0 – the concentration of the MK2 / pepMK2 at the given point,

K_0 – the constant concentration of the p38,

K_d – the dissociation constant of the two interacting partners.

S7. K_d of p38^{C162S} and pepMK2

A slight difference was recorded between literature data (50 nM for p38^{wt} and CF-pepMK2^{wt} in FP buffer) and our K_d value obtained by FRET (240 nM in PBS) for Cy1-labeled p38^{C162S} and Cy3-conjugated pepMK2. The difference between those values is attributed to several alterations between the conditions of the two measurements:

(i) the method: fluorescence polarization vs. FRET efficiency
(ii) the buffer composition including pH and ionic strength: FP buffer [20 mM Tris (pH 8.0), 100 mM NaCl, 0.05% Brij35P, and 2 mM DTT] vs. PBS [10 mM Na_2HPO_4, 1.8 mM KH_2PO_4, 137 mM NaCl, 2.7 mM KCl, (pH7.4)]
(iii) the labeling fluorophore: fluorescein at N-terminal amino group vs. Cy3 on thiol group at N-terminal Cys
(iv) the AA composition of the protein at position 162 (in docking site) wild type: Cys vs. mutant: Ser
(v) the peptide sequence: IKIKKIEDASNPLLLKRRKK vs **CQ**IKIKKIEDASNPLLLKRRKK.

In order to assess the background of the differences between K_d values we measured several combinations of wild type and mutant protein with the peptide in different buffers with an orthogonal method. While the changes in fluorescent intensity of Cy3-pepMK2 were proportional to the concentration of the protein we estimated dissociation constants based on this titration.
The K_d value for unlabeled p38^{wt} with Cy3-conjugated pepMK2 in FP and PBS buffer was 175 nM (not shown) and 314 nM, respectively (Fig. S14a). Accordingly, not only the buffer composition can alter the affinity but the additional CQ amino acids at the N-terminal of the peptide increased the dissociation constant compared to the literature data (50 nM). K_d for unlabeled mutant p38^{C162S} and Cy3-conjugated pepMK2 in PBS was 96 nM (Fig. S14b) and after labeling p38^{C162S} with Cy1 the same constant was 49 nM (Fig. S14c). In summary, the association of p38 and MK2 peptide could slightly differ if we changed the composition, the ionic strength and pH of the buffer as well as it depended on the measuring method, the peptide sequence and the labeling fluorophore and moreover the type of protein residue at 162 position.

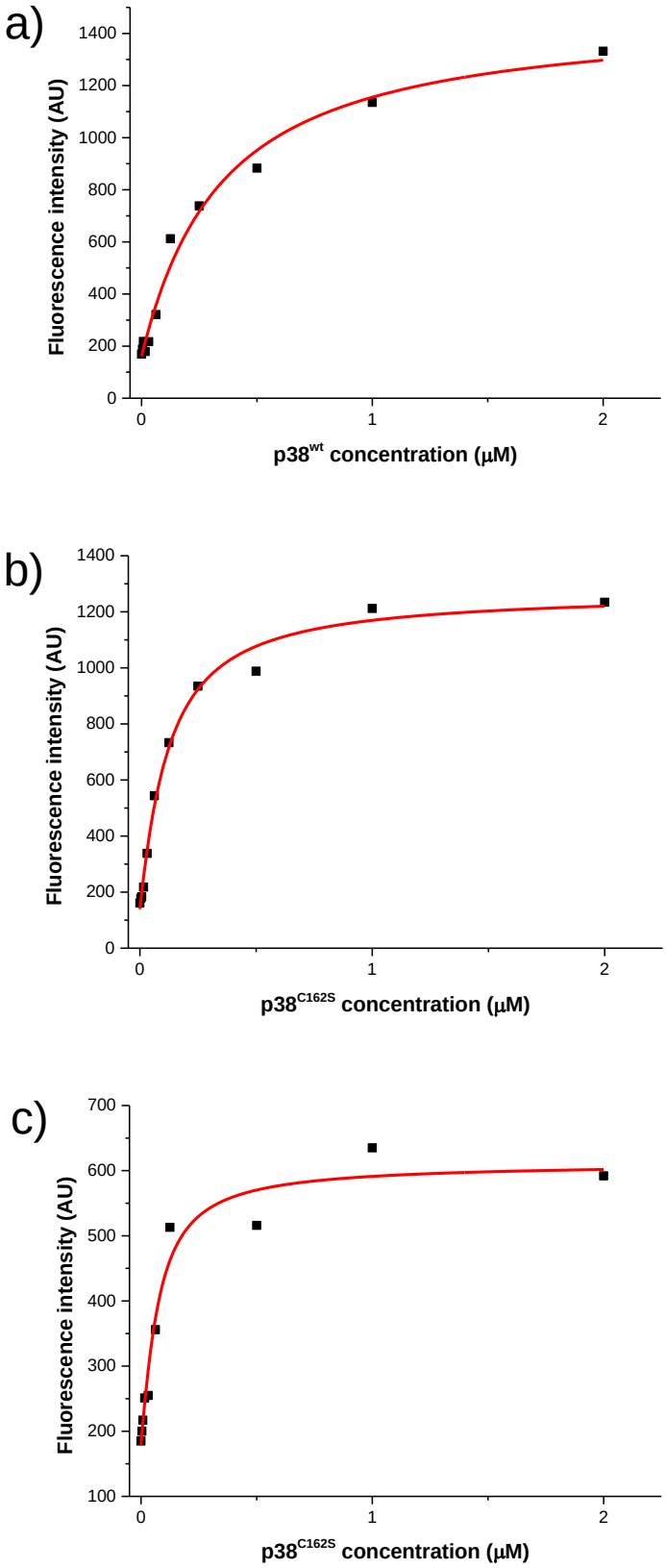

Fig. S14. Binding of unlabeled p38^{wt} (**a**) or unlabeled (**b**) and Cy1-conjugated (**c**) p38^{C162S} to Cy3-pepMK2.

S8. Protein-protein FRET measurements

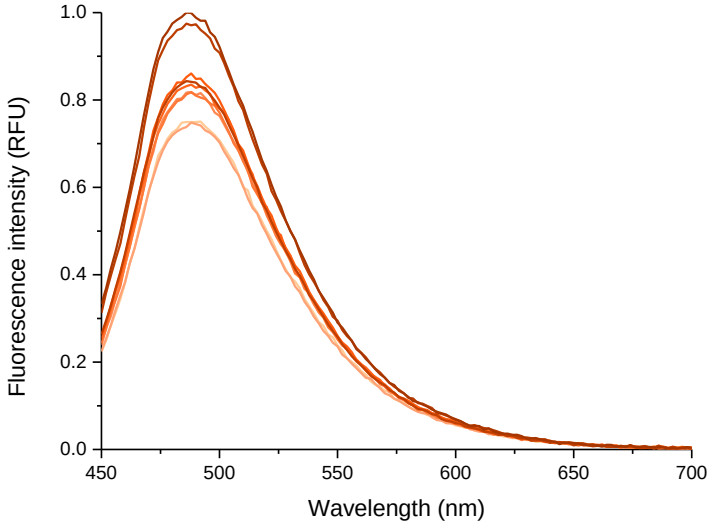

Fig S15. Fluorescence intensity of the Cy1-labeled $p38^{C162S}$ in the presence of unlabeled MK2 at the respective concentrations.

S9. Characterization of the compounds

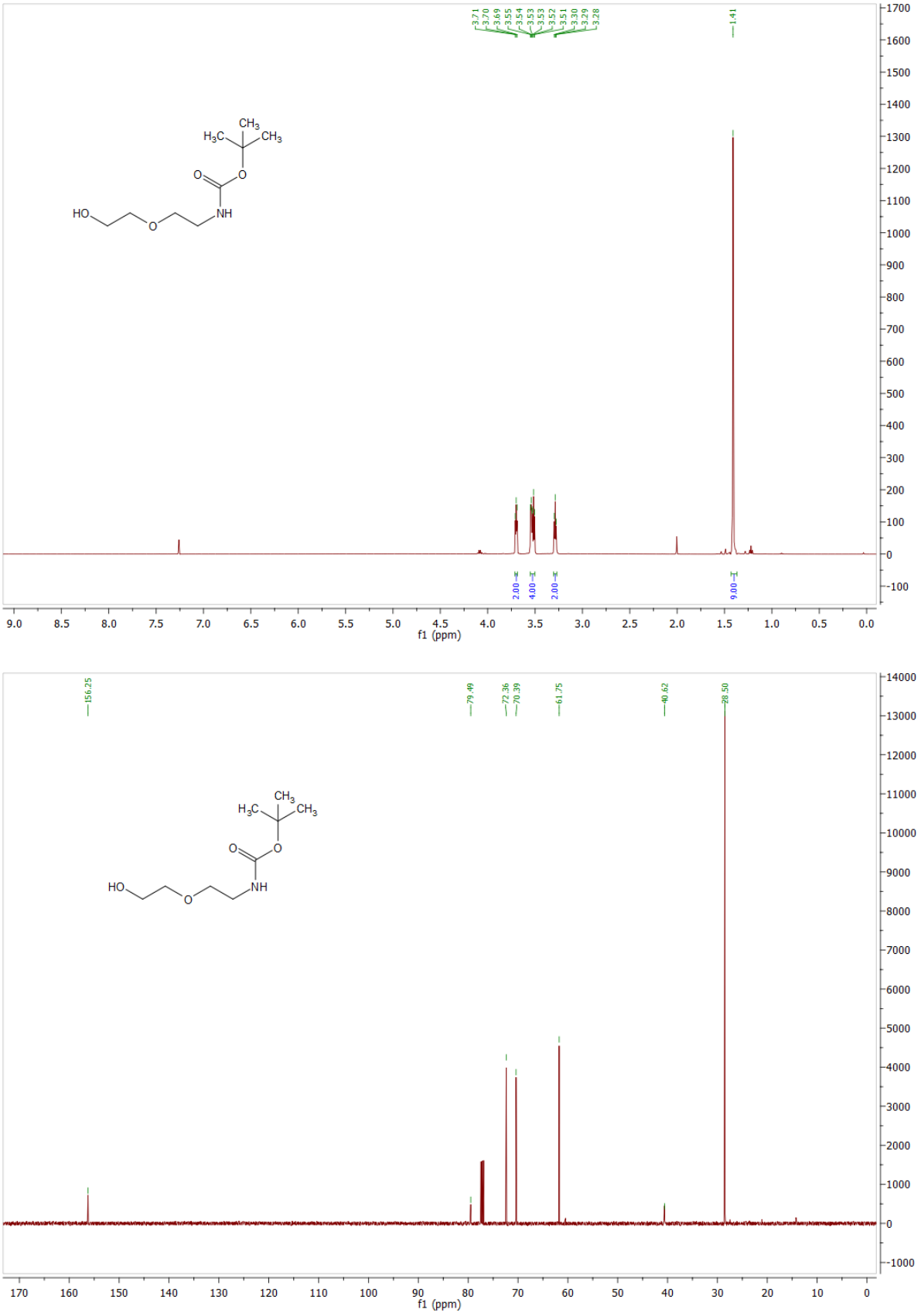

Fig S16. ^{1}H and ^{13}C NMR spectra of tert-butyl (2-(2-hydroxyethoxy)ethyl)carbamate (**2**).

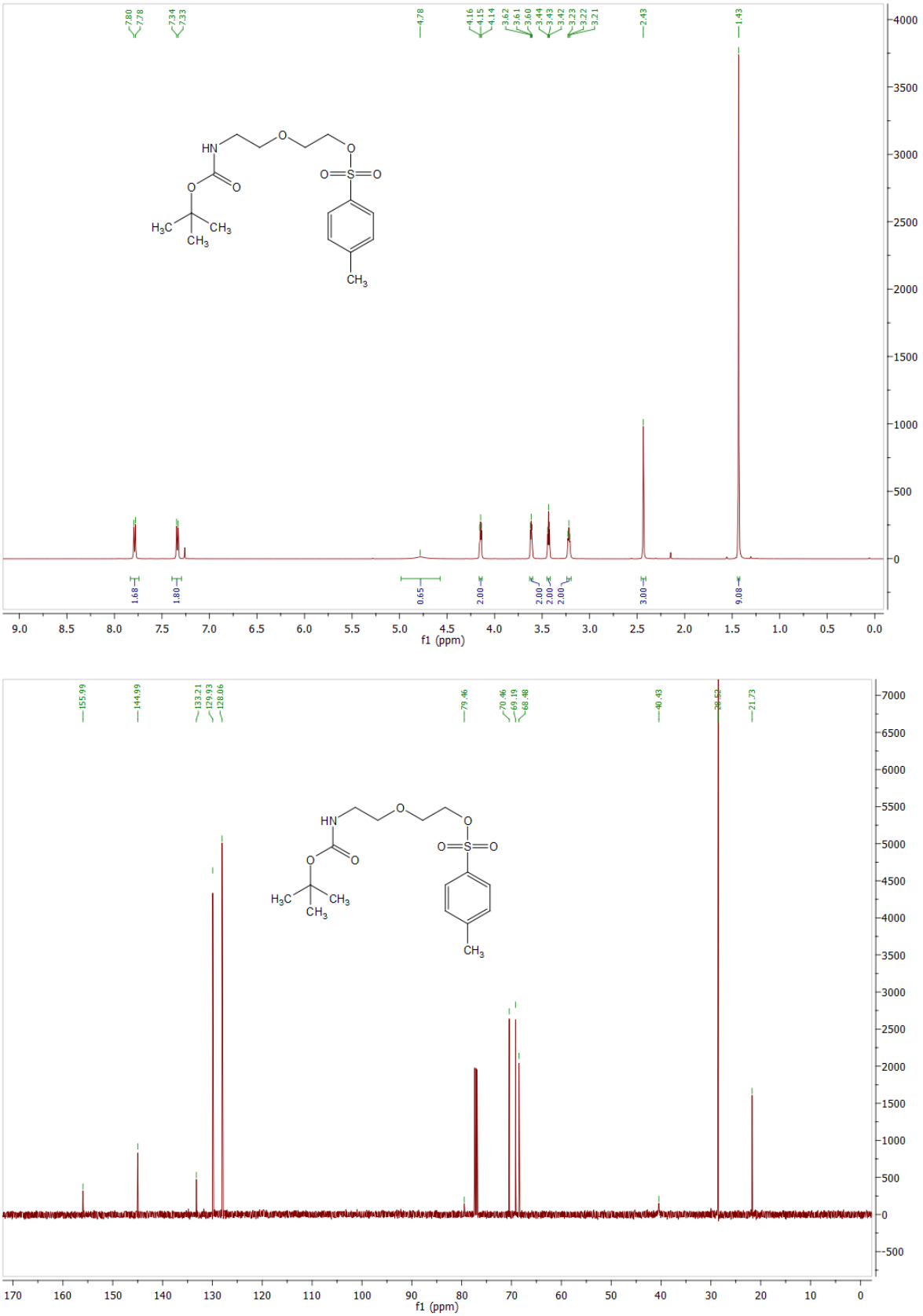

Fig S17. ^{1}H and ^{13}C NMR spectra 2-(2-((tert-butoxycarbonyl)amino)ethoxy)ethyl 4-methylbenzenesulfonate (**3**).

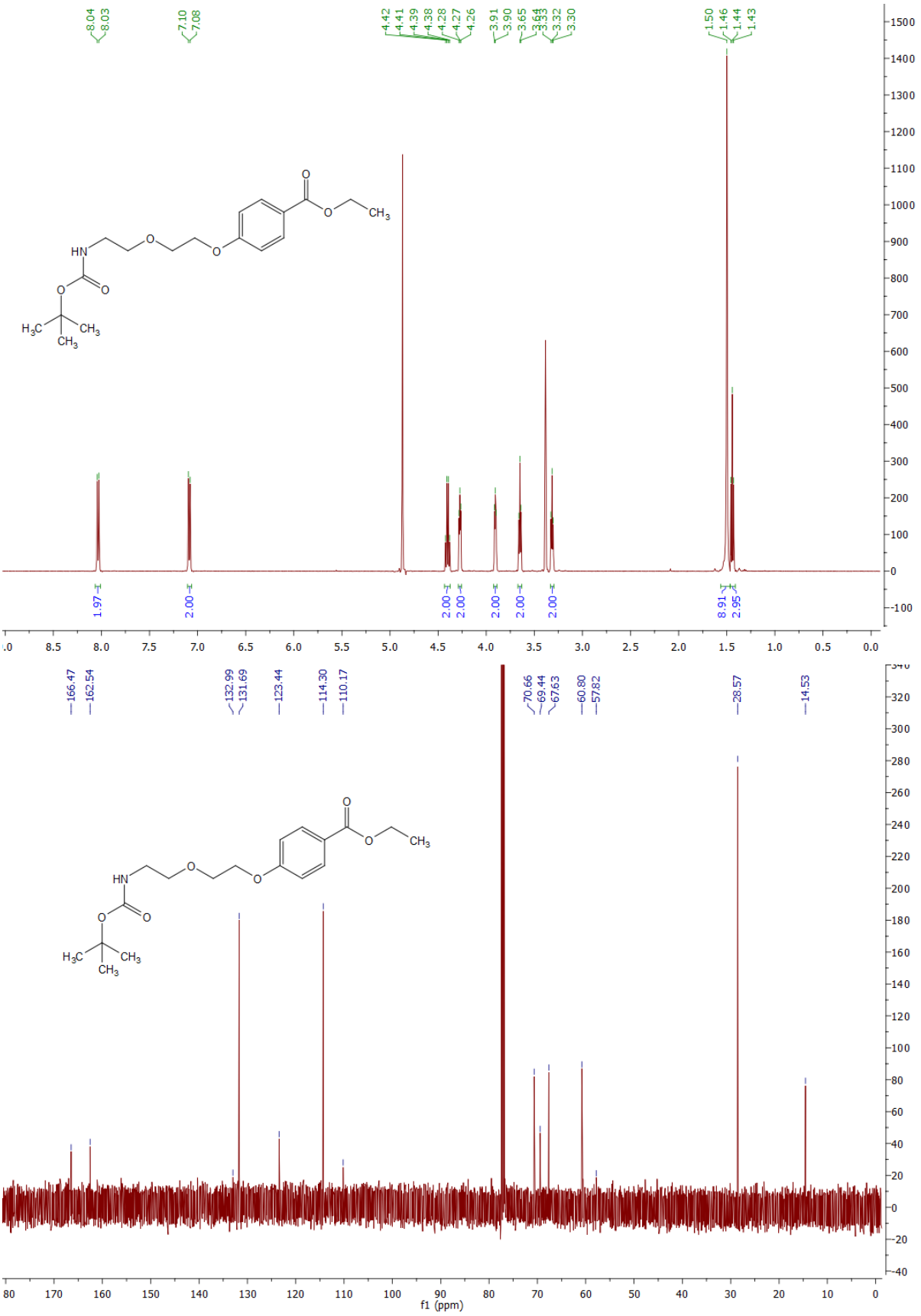

Fig S18. ^{1}H and ^{13}C NMR spectra of ethyl 4-(2-(2-((tert-butoxycarbonyl)-amino)ethoxy)ethoxy)benzoate (**4**).

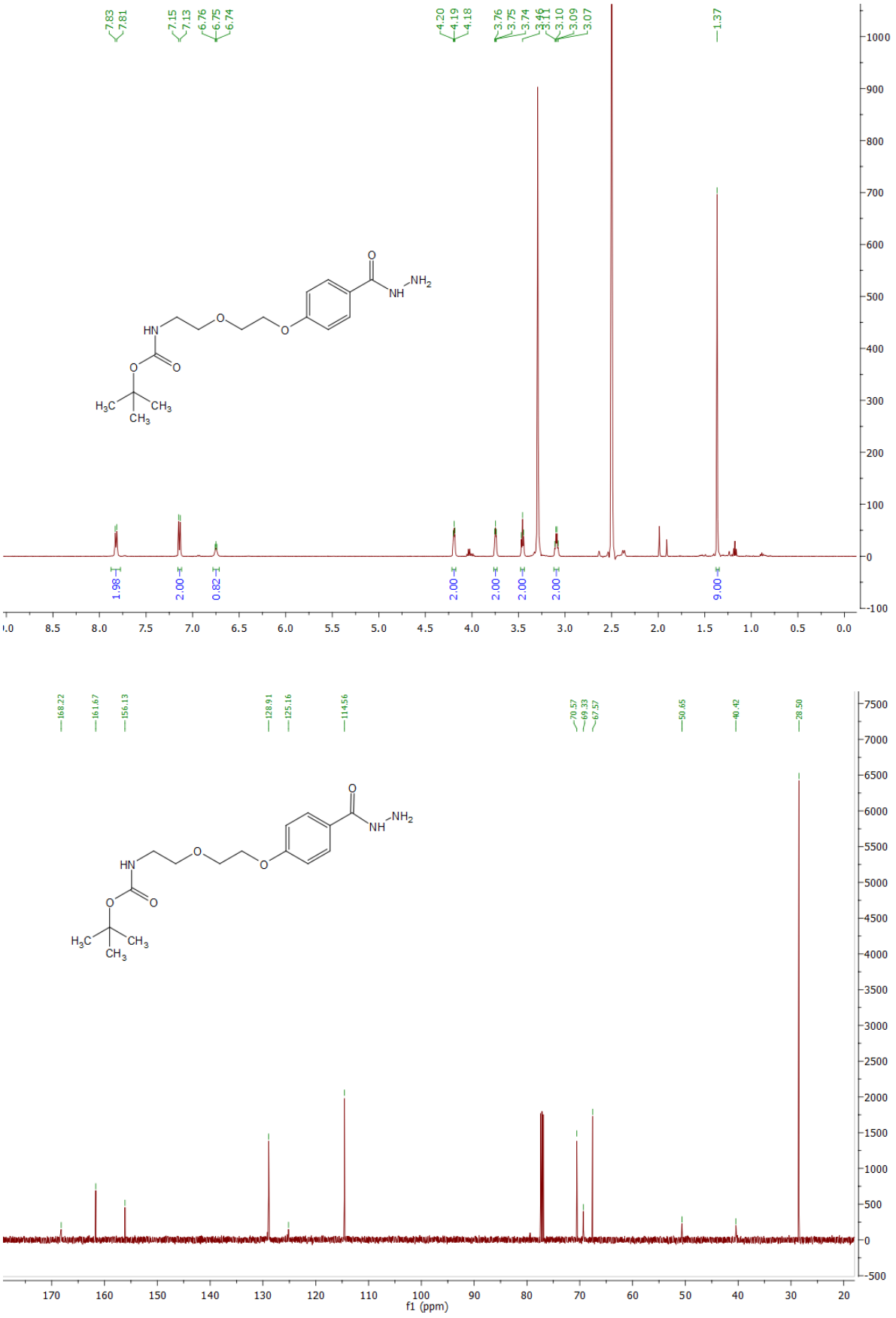

Fig S19. ^{1}H and ^{13}C NMR spectra of tert-butyl (2-(2-(4-(hydrazinecarbonyl)phenoxy)ethoxy)ethyl)carbamate (**5**).

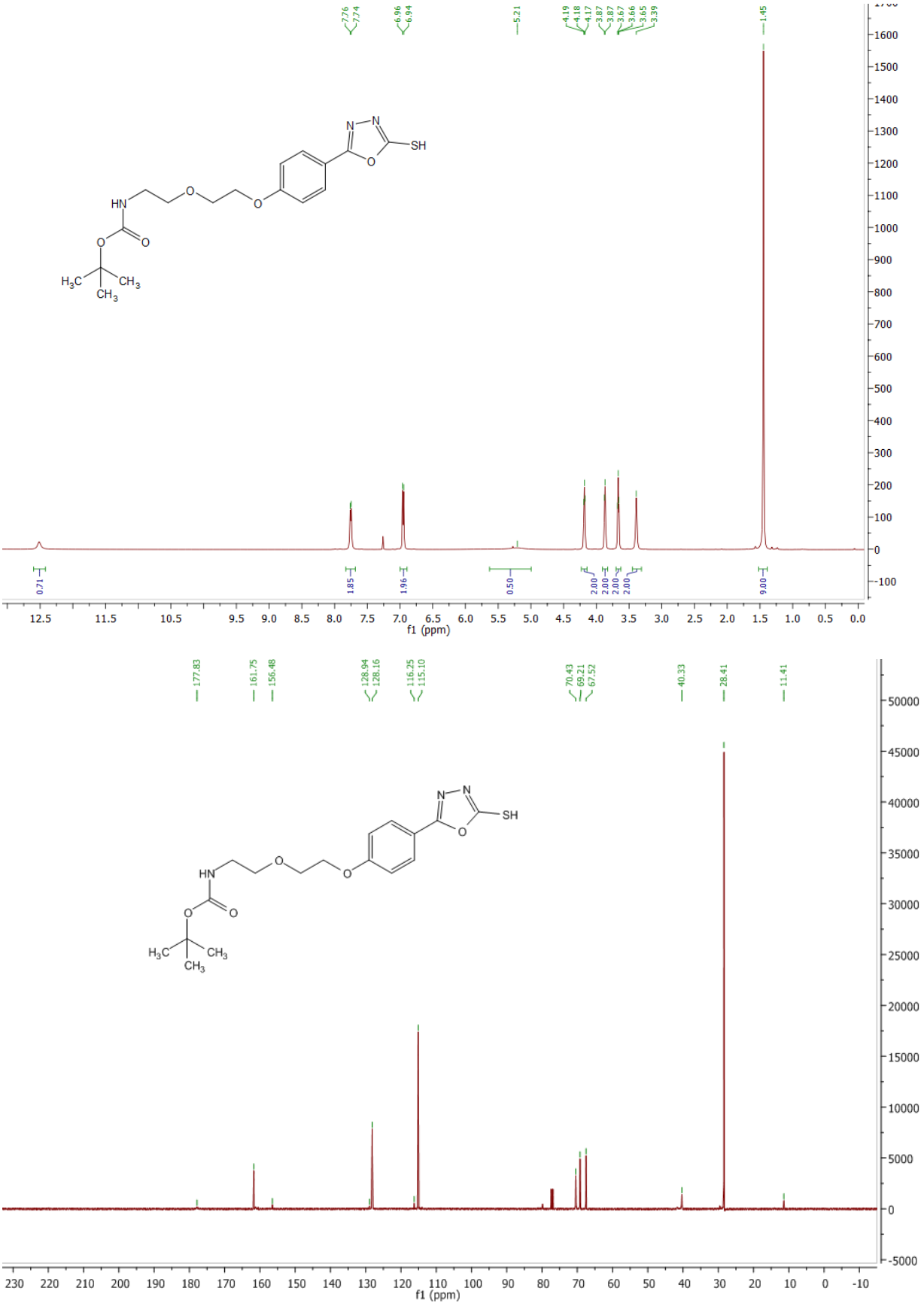

Fig S20. ^{1}H and ^{13}C NMR spectra of tert-butyl (2-(2-(4-(5-mercapto-1,3,4-oxadiazol-2-yl)phenoxy)ethoxy)ethyl)carbamate (**6**).

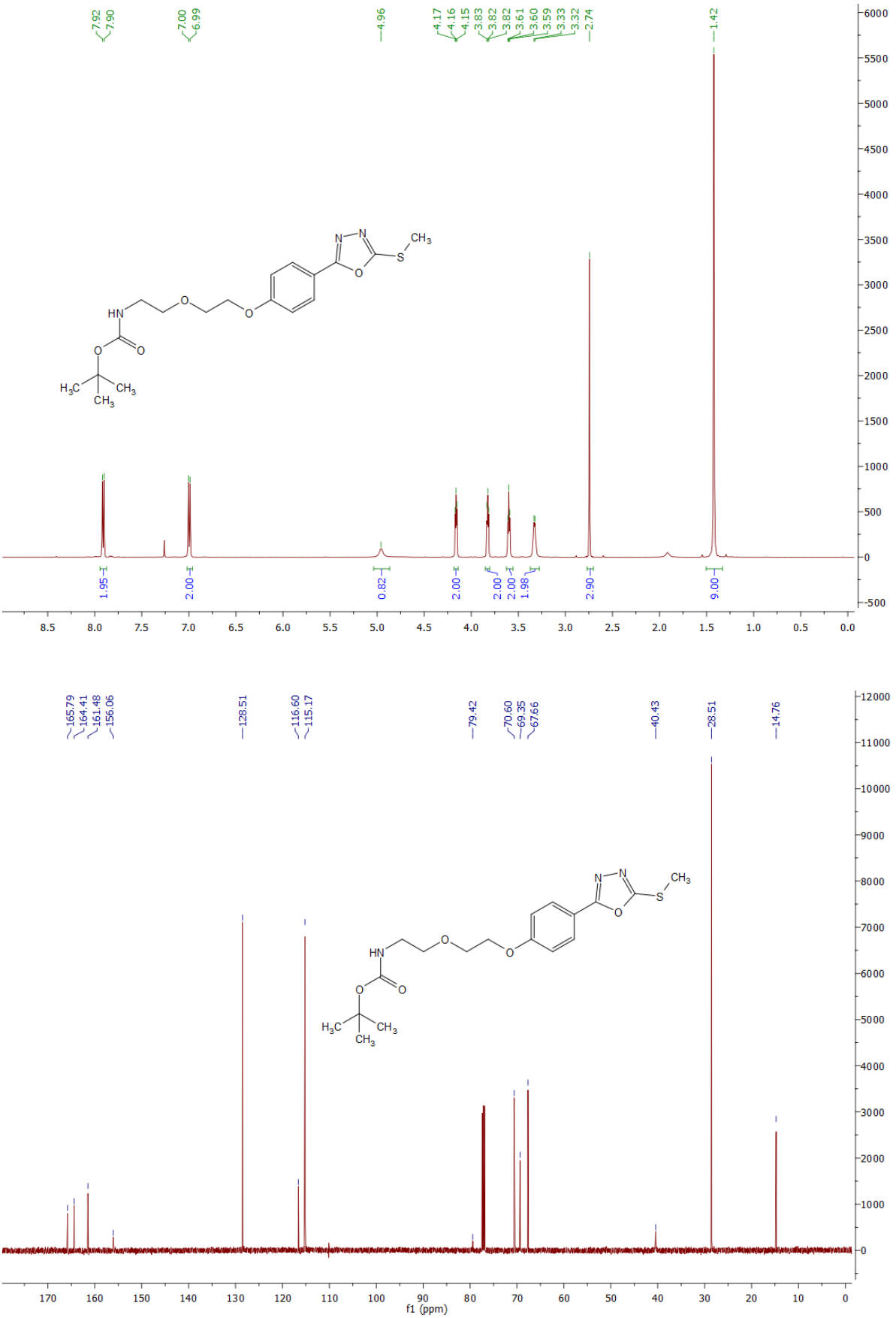

Fig S21. ^{1}H and ^{13}C NMR spectra of tert-butyl (2-(2-(4-(5-(methylthio)-1,3,4-oxadiazol-2-yl)phenoxy)ethoxy)ethyl)carbamate (**7**).

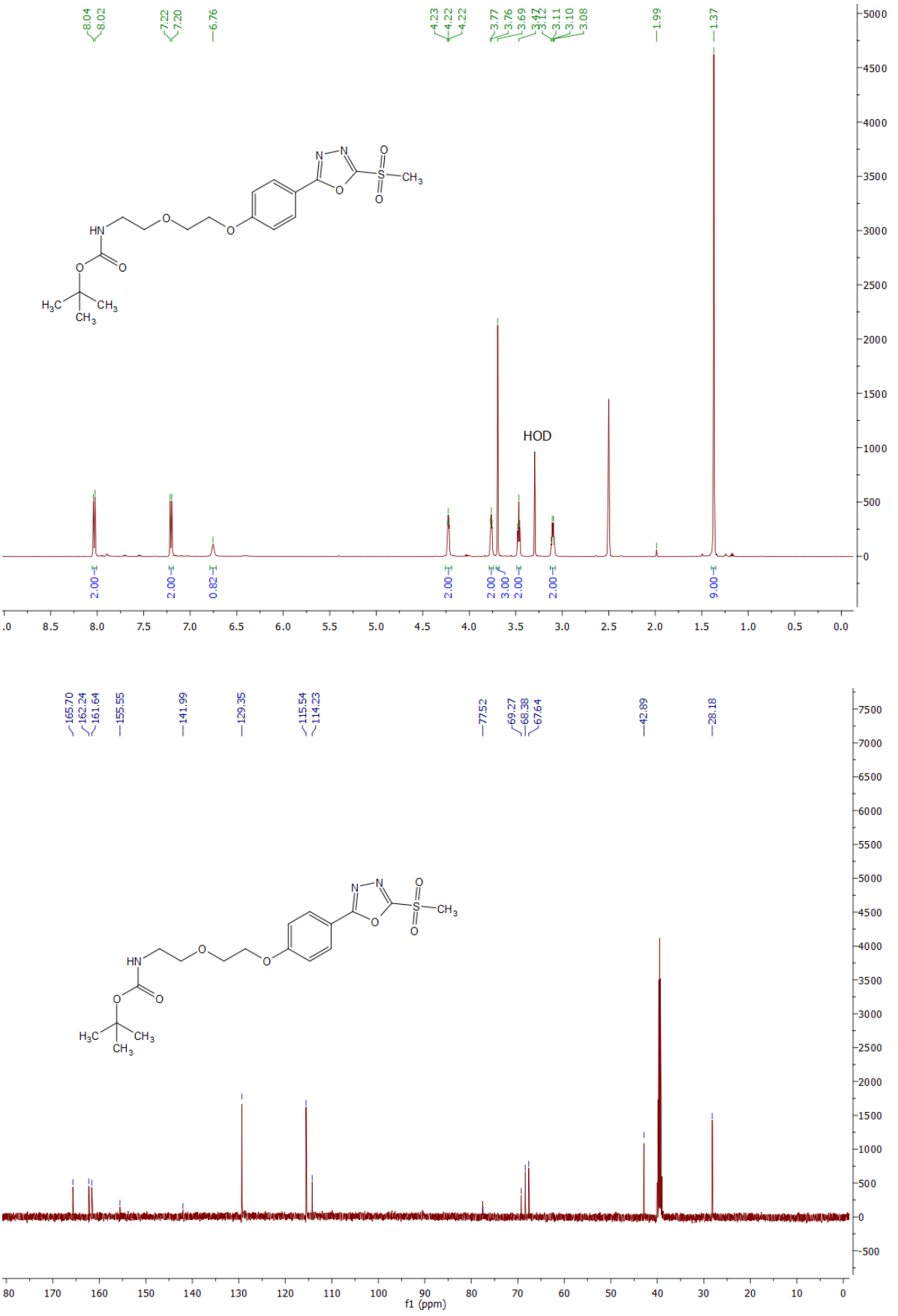

Fig S22. ^{1}H and ^{13}C NMR spectra of tert-butyl (2-(2-(4-(5-(methylsulfonyl)-1,3,4-oxadiazol-2-yl)phenoxy)ethoxy)ethyl)carbamate (**8**).

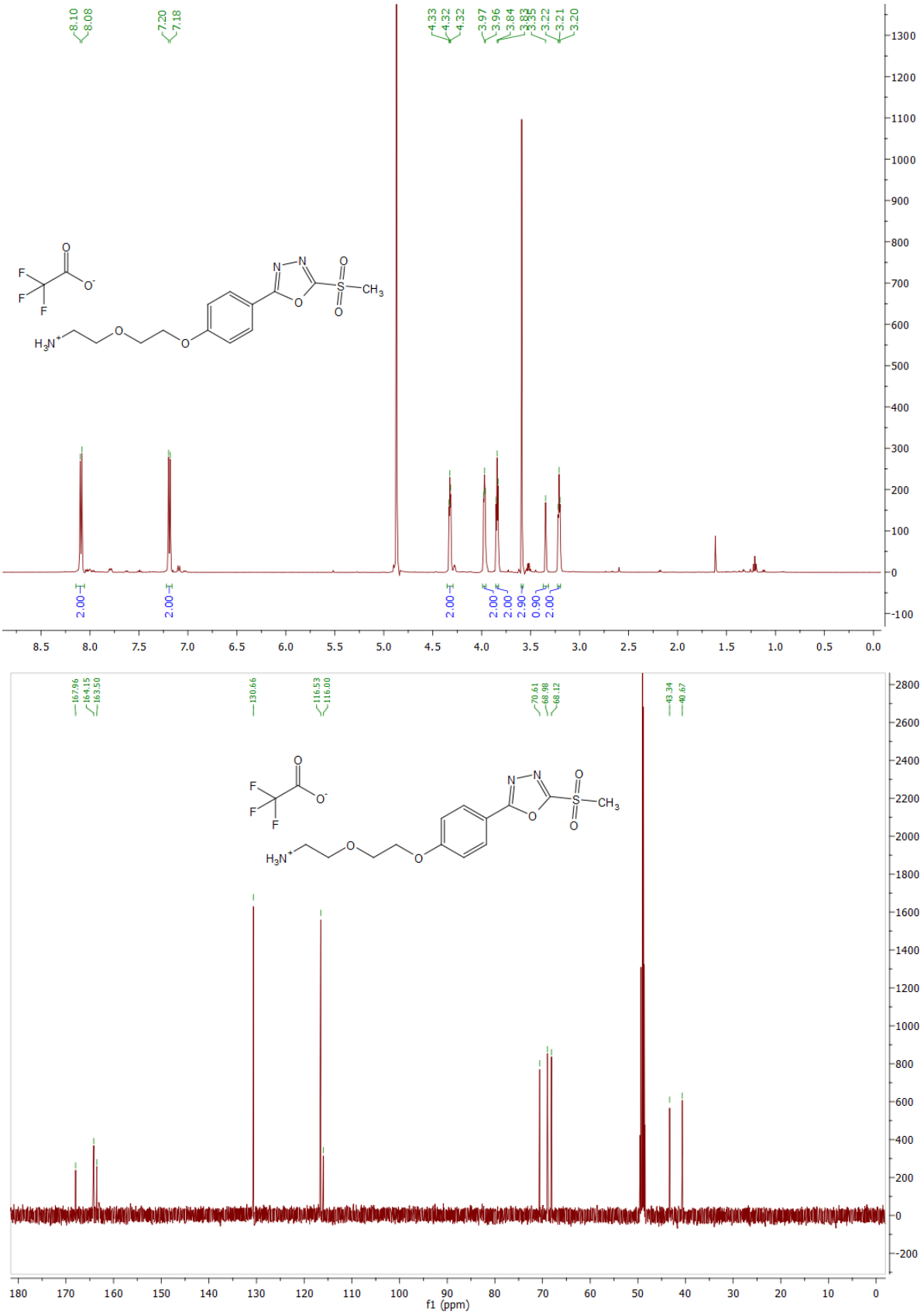

Fig S23. ^{1}H and ^{13}C NMR spectra of 2-(2-(4-(5-(methylsulfonyl)-1,3,4-oxadiazol-2-yl)phenoxy)ethoxy)ethan-1-aminium 2,2,2-trifluoroacetate (**9**).

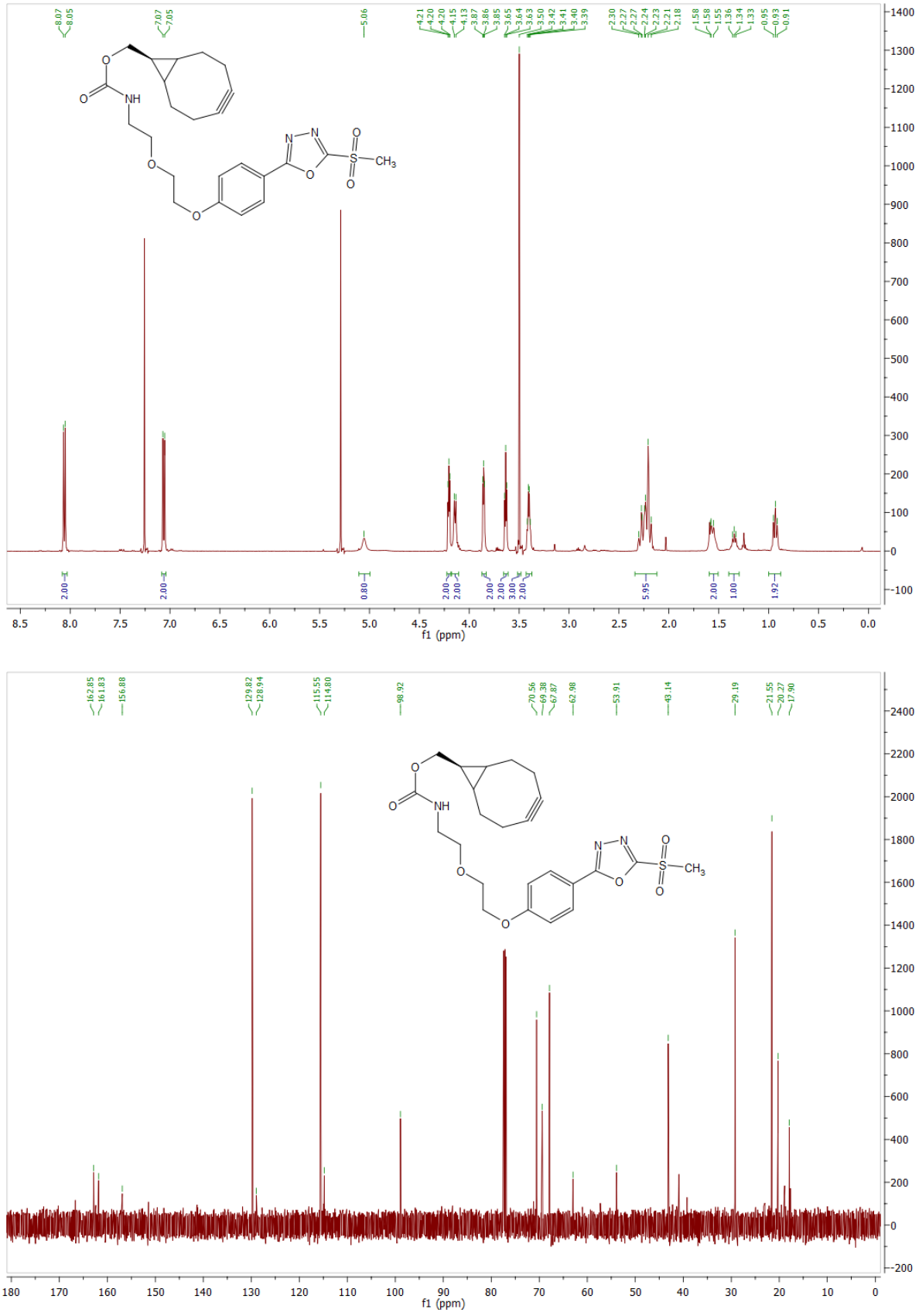

Fig S24. ^{1}H and ^{13}C NMR spectra of bicyclo[6.1.0]non-4-yn-9-ylmethyl (2-(2-(4-(5-(methylsulfonyl)-1,3,4-oxadiazol-2-yl)phenoxy)ethoxy)ethyl)carbamate (**10**).

S10. References

1. T. Imre, G. Schlosser, G. Pocsfalvi, R. Siciliano, É. Molnár-Szöllősi, T. Kremmer, A. Malorni, K. Vékey, *J. Mass Spectrom.*, 2005, **40**, 1472–1483.